Electronic Supplementary Material (ESI) for Journal of Materials Chemistry A.

Supporting Information

Beetle and Cactus-Inspired Surface Endows Continuous and Directional Droplet Jumping for Efficient Water Harvesting

Xikui Wang[1,3], Jia Zeng[1], Jing Li[2], Xinquan Yu[1], Zuankai Wang[2]* and Youfa Zhang[1]*

1. Jiangsu Key Laboratory of Advanced Metallic Materials, School of Materials Science and Engineering, Southeast University, Nanjing 211189, China

2. Department of Mechanical Engineering, City University of Hong Kong, Hong Kong 999077, China

School of Electrical and Mechanical Engineering, Pingdingshan University, Pingdingshan 467000, PR China

*E-mail: zuanwang@cityu.edu.hk(Z.W.); yfzhang@seu.edu.cn (Y.Z.)

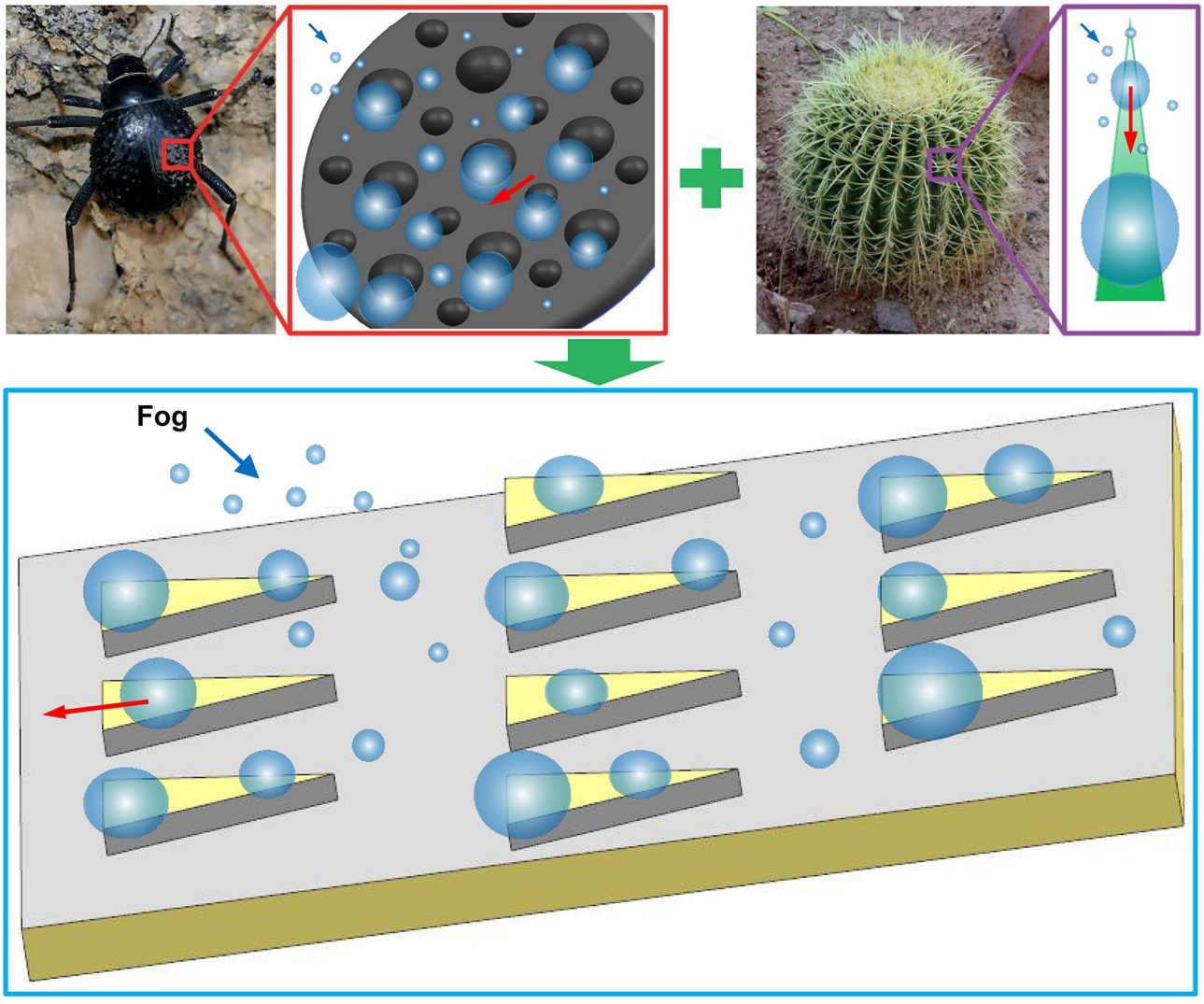

Fig. S1 Design strategy of patterned surface inspired by Namib desert beetles and cactus thorns. Approximate species dimensions are: desert beetle, 1.5 cm long; cactus, 20 cm in diameter[1].

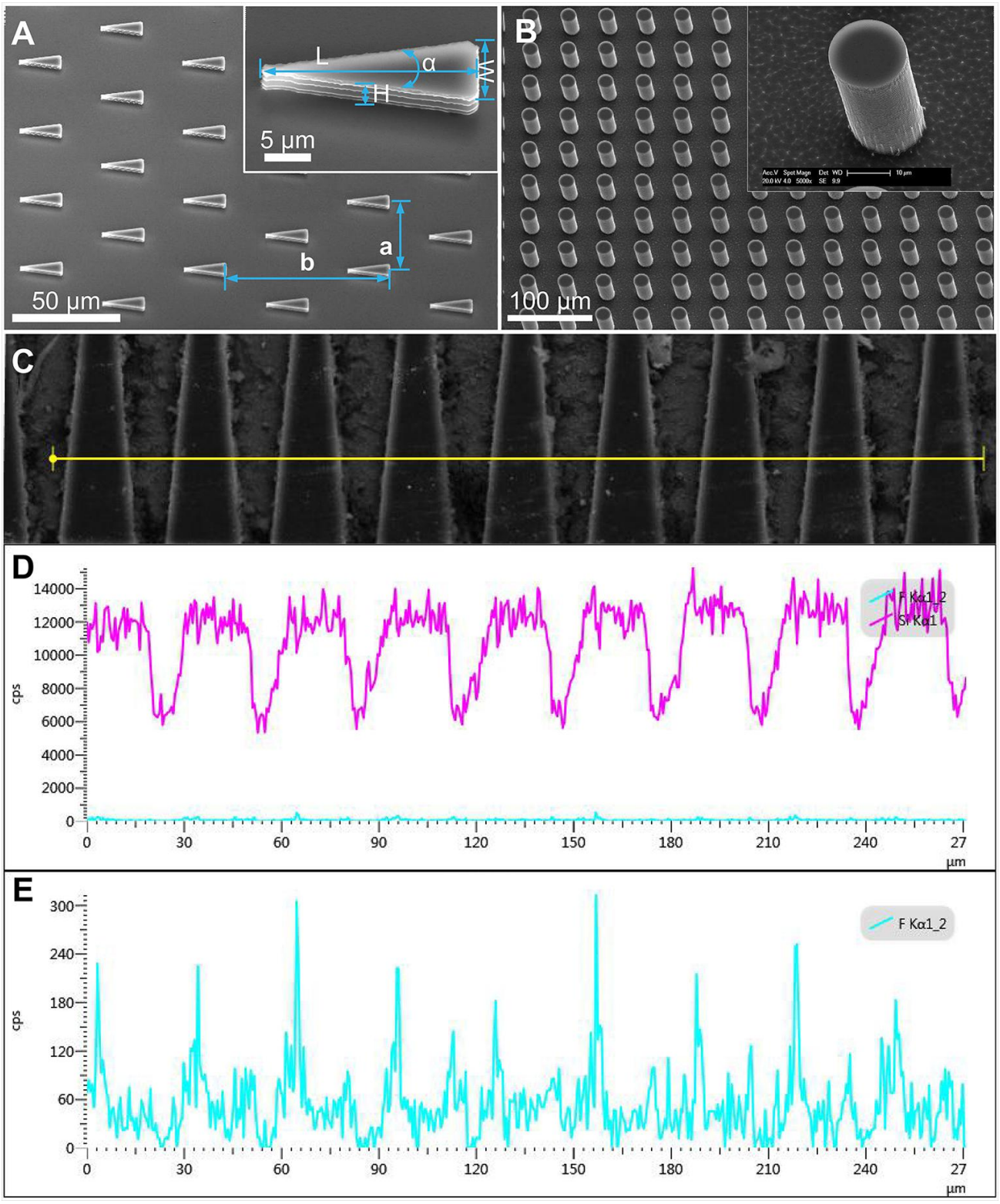

Fig. S2 SEM images of bump arrays and elements distribution on the hybrid wetting patterned surface. (A) SEM image of wedge-shaped silicon bump arrays (α=20°, W=10 μm, L=28.4 μm, a=56.8 μm, b=96.8 μm, H=5 μm), the top insets show the SEM image of a single bump. (B) SEM image of cylindrical pillar arrays. (C) SEM image of the Dense-BCI surface. (D) Element distribution of Si and F. (E) Element distribution of F. The images show that the elements of F and Si on the hybrid wetting patterned surface are heterogeneous, and the top surfaces of the bumps have less F and more Si than the Nanocoating surface.

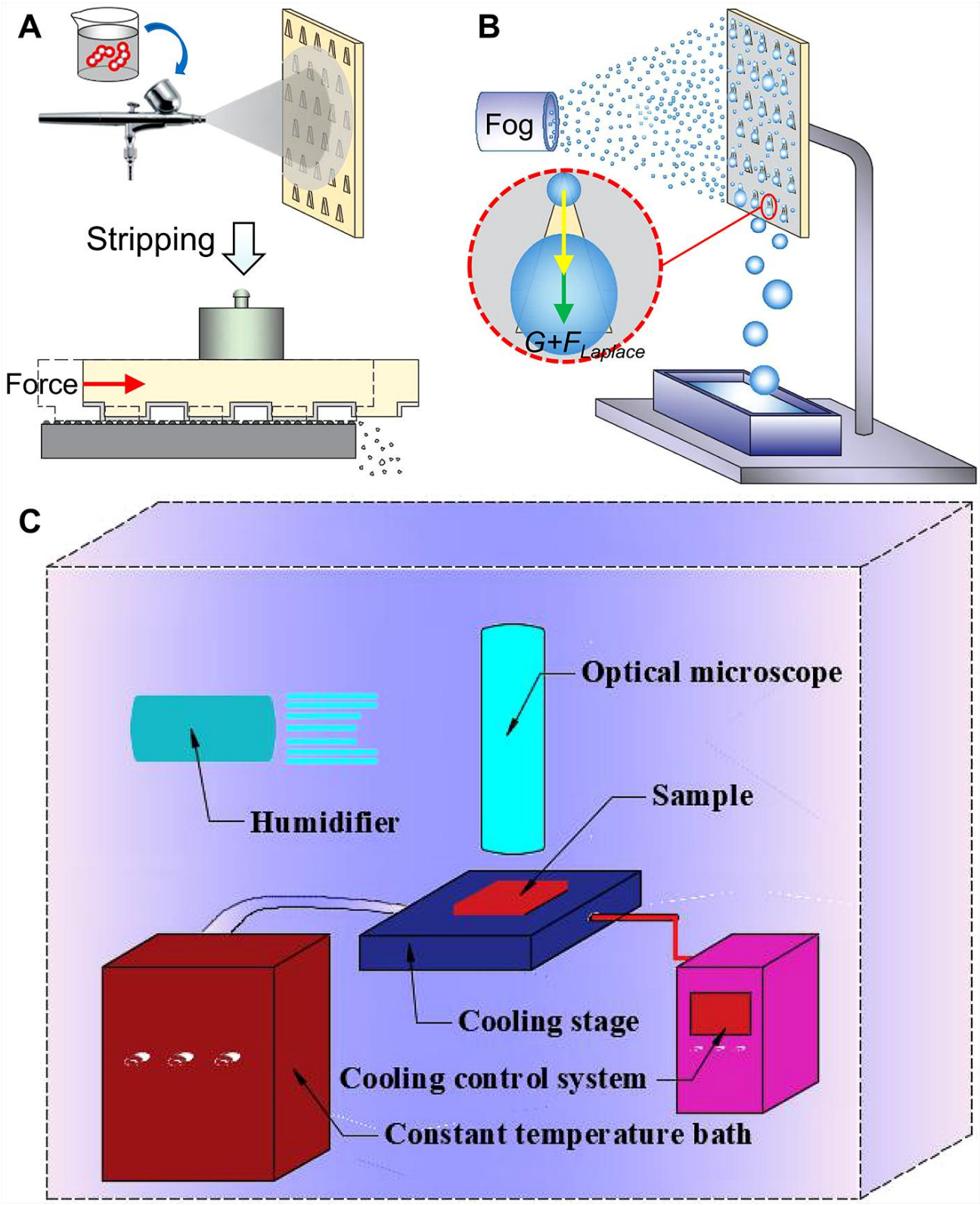

Fig. S3 Illustration of the experimental process. (A) Preparation process of the patterned hybrid wetting surface with wedge-shaped bumps. (B) Home-made water collection device. (C) Illustration of the condensation test system.

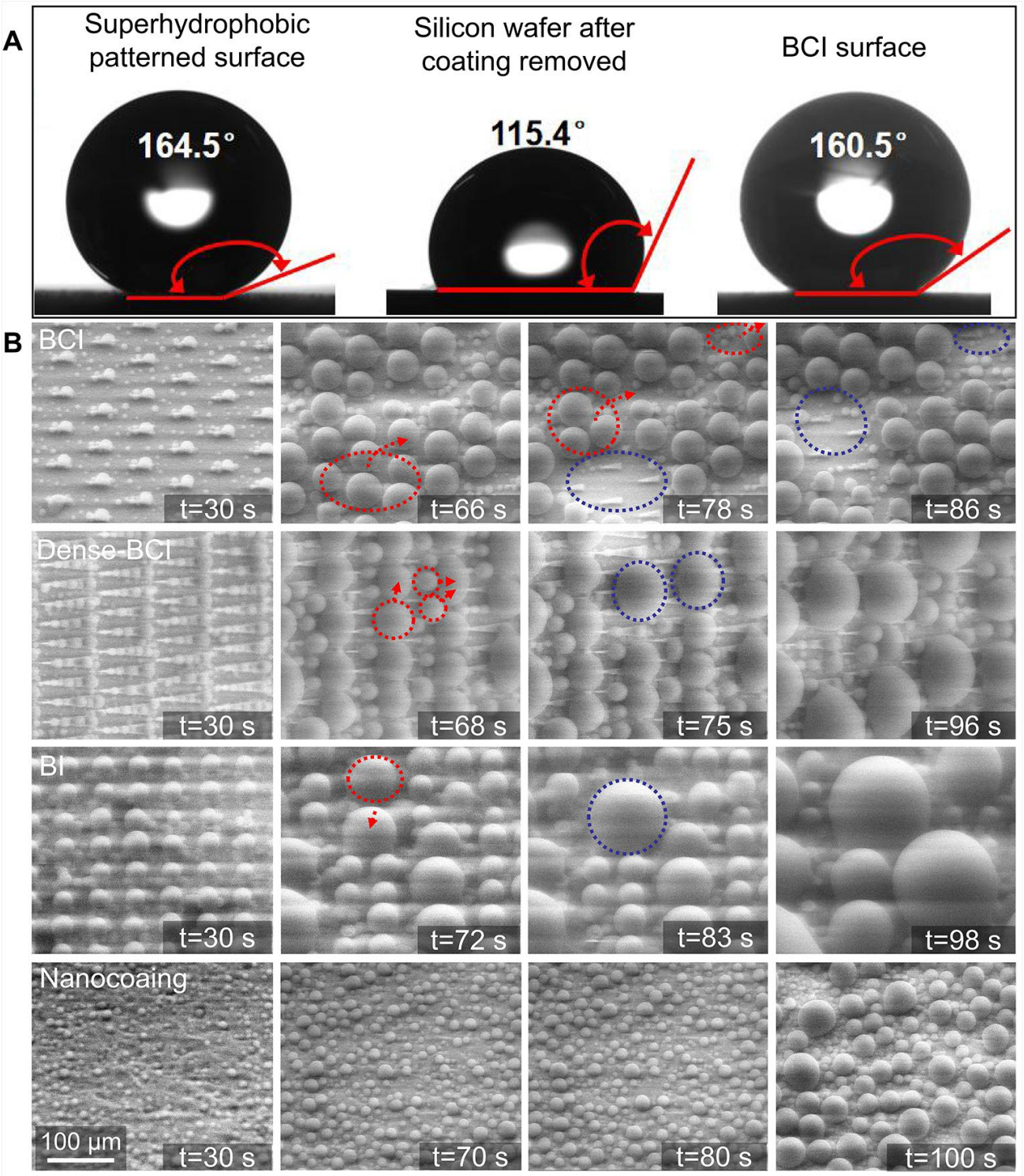

Fig. S4 Surface wettability and dropwise condensation performance for different surfaces. (A) Water contact angles of different surfaces. (B) Dropwise condensation and droplets growth on different surfaces (the field of view is ~320 μm×~370 μm).

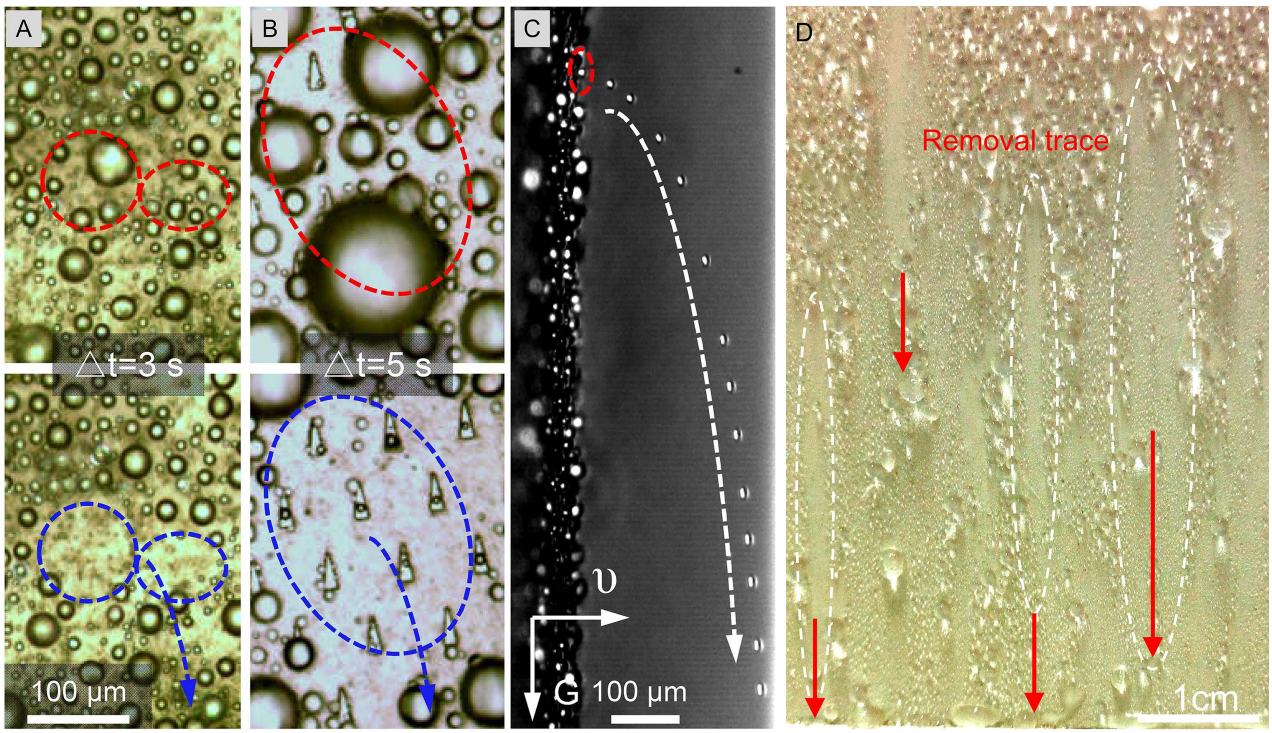

Fig. S5 Droplets departure from the Nanocoating surface and the BCI surface in the vertical direction. (A) coalescence and departure from the Nanocoating surface. (B) Drops coalescence and departure from the BCI surface. (C) The track images of drop departure from the BCI surface in the vertical direction with the wedge-shaped tip upwards. (D) Droplets are removed by gravity from a control sample surface and leave a removal trace (the surface coated with a hybrid coating mixed with silicon carbide and superhydrophobic SiO_2 nanoparticles).

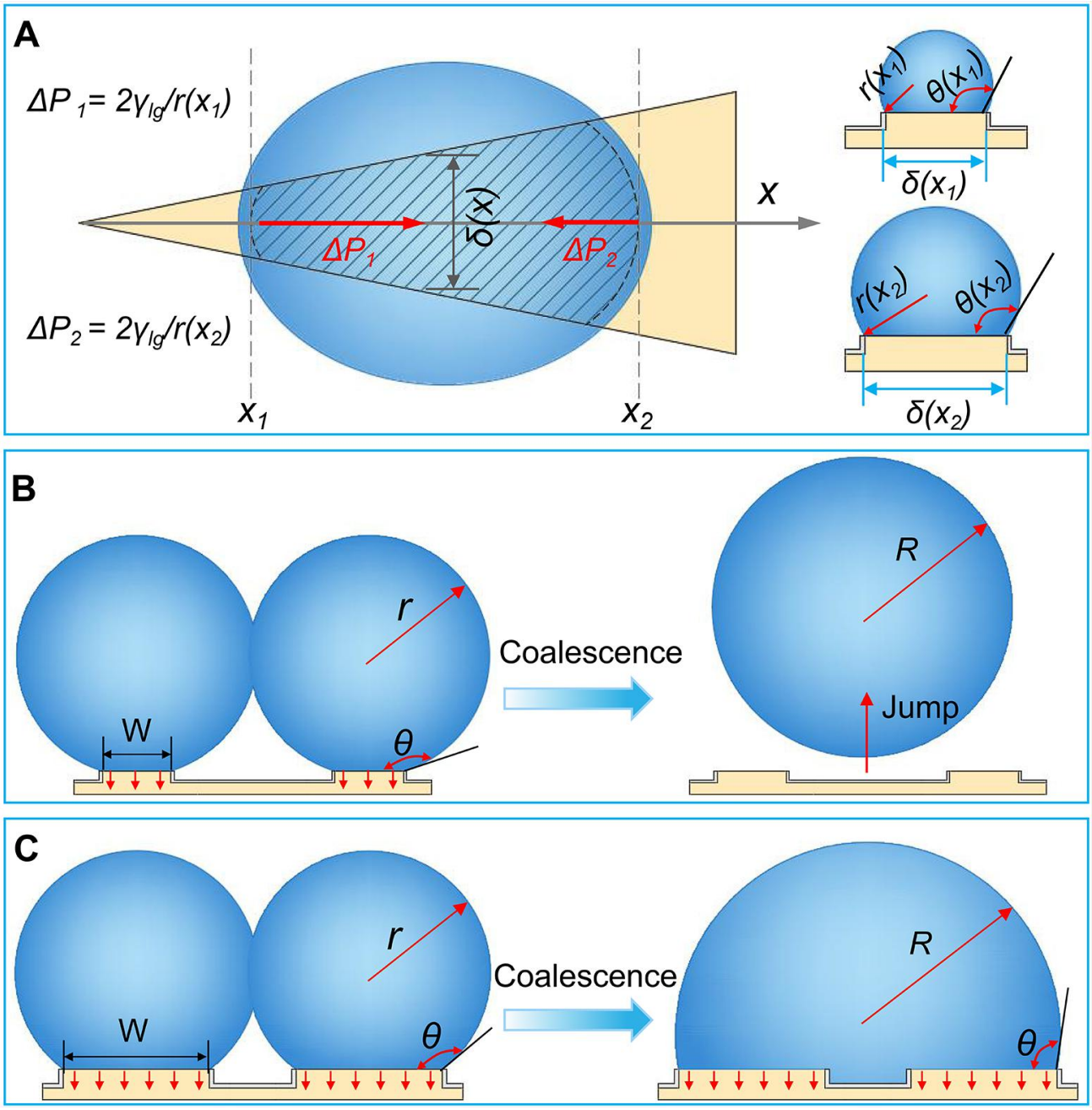

Fig. S6 Force analysis and jumping mechanism on different surfaces. (A) Force analysis of droplet on the top surface of the wedge-shaped bump. (B) Droplets coalescence and jumping behaviour on the BCI surface (α=20°, W=10 μm, L=28.4 μm, a=56.8 μm, b=96.8 μm and H=5 μm). (C) Droplets coalescence behaviour on the Dense-BCI surface (α=10°, W=20 μm, L=114.3 μm, a=30.6 μm, b=248.6 μm and H=5 μm).

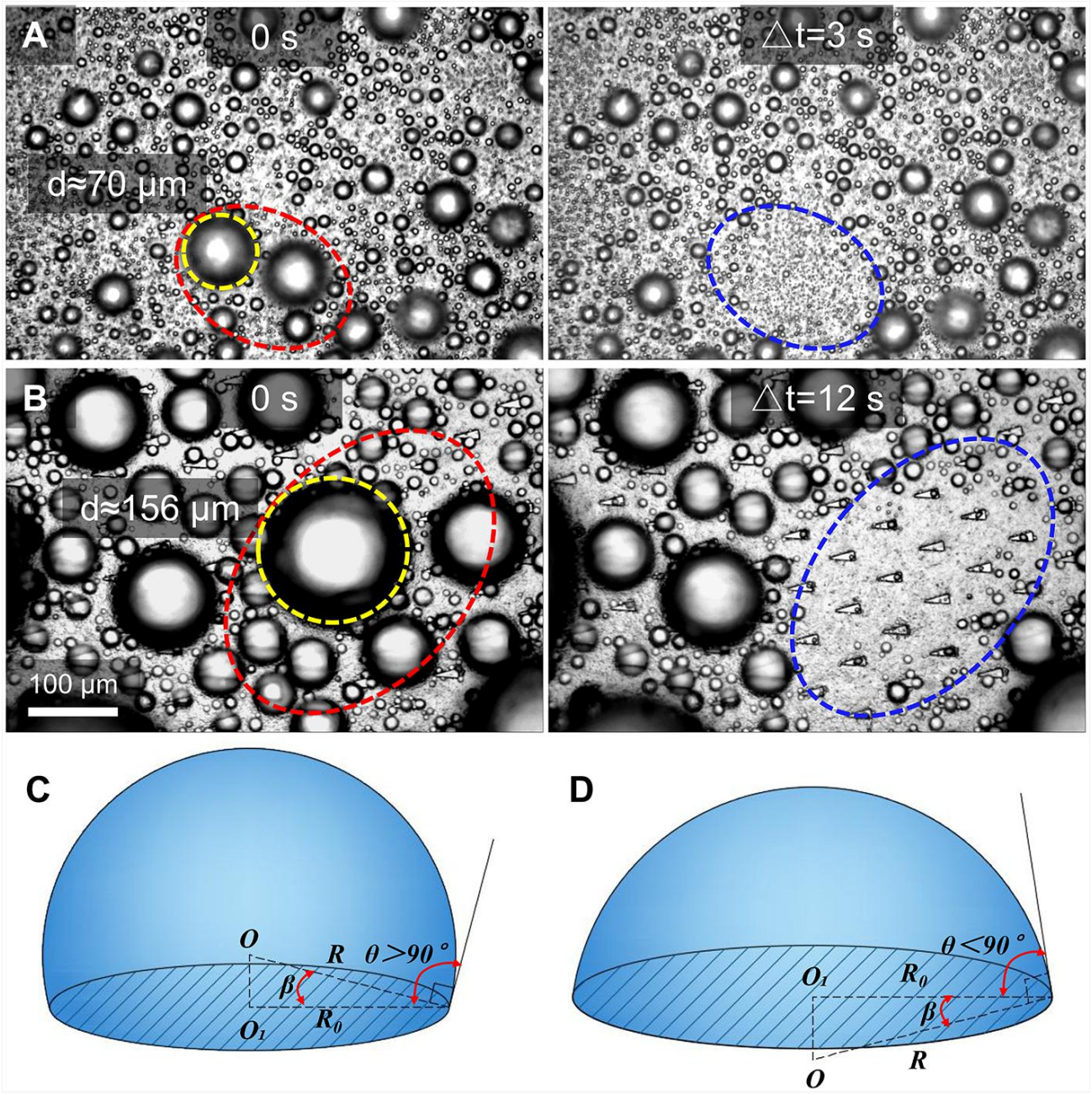

Fig. S7 Self-repelled droplets jumping of different surface and droplet contact angle on the bump's top surface. (A) Droplets coalescence and departure from the Nanocoating surface. (B) Droplets coalescence and departure from the BCI surface. The results show that the total volume of the droplet departure from the Nanocoating surface was only ~5.20×10^5 μm^3, while the total volume of the droplet departure from the BCI surface was ~3.80×10^6 μm^3, which equivalent to ~7.3 times for that of the Nanocoating surface. (C) Contact angle of $\theta>90°$. D) Contact angle of $\theta<90°$.

The work of adhesion (E_w) for one drop can be expressed by the following formula[2,3]:

$$E_w = \pi\gamma_{lv}R^2(1+cos\theta)\ \ sin^2\theta \qquad \text{S1}$$

In order to calculate the adhesion work for per unit of contact area (E_{w0}), the circle radius of the contact area (R_0) could be scaled as:

$$R_0 = R\cos\beta \quad \text{S2}$$

$$\beta = \theta - 90°(90° < \theta < 180°) \text{ or } \beta = 90° - \theta \ (0° < \theta < 90°) \quad \text{S3}$$

Then, R_0 could be expressed as:

$$R_0 = R\sin\theta \quad \text{S4}$$

The contact area (S_0) of the drop could be expressed as:

$$S_0 = \pi R_0^2 = \pi R^2 \sin^2\theta \quad \text{S5}$$

Therefore, the work of adhesion for per unit of contact area (E_{w0}) is:

$$E_{w0} = \frac{E_w}{S_0} = \frac{\pi\gamma_{lv}R^2(1+\cos\theta)\sin^2\theta}{\pi R^2\sin^2\theta} = \gamma_{lv}(1+\cos\theta) \quad \text{S6}$$

The surface energy (E_s) of droplet after coalesced can be expressed as[4]:

$$E_s \approx \Delta A\gamma_{lv} \quad \text{S7}$$

The viscous dissipation (E_{vis0}) for one droplet is described as[2]:

$$E_{vis0} \approx 36\pi\mu\sqrt{\frac{\gamma_{lv}r^3}{\rho}} \quad \text{S8}$$

Hence, the total viscous dissipation (E_{vis}) for multiple droplets is described as:

$$E_{vis} \approx \sum_{i=1}^{n} 36\pi\mu\sqrt{\frac{\gamma_{lv}r_i^3}{\rho}} (n \geq 2) \quad \text{S9}$$

Similarly, the total surface adhesion work for multiple droplets can be described as:

$$E_w \approx \sum_{i=1}^{n} A_i\gamma_{lv}(1+\cos\theta)(n \geq 2) \quad \text{S10}$$

Where A_i represents the solid-liquid contact area between water droplets and the bum.

Table S1 The experimental results in this paper compared with SAB[1] and MATS[5]

Sample	diameter (μm)	Water collection rate (g/m^2/h)	Jumping distance (μm)
BCI	106±25～365±84	~11862.2	351±112～4097±291
MATS	14±2～63±11	/	/
SAB	/	~90	/

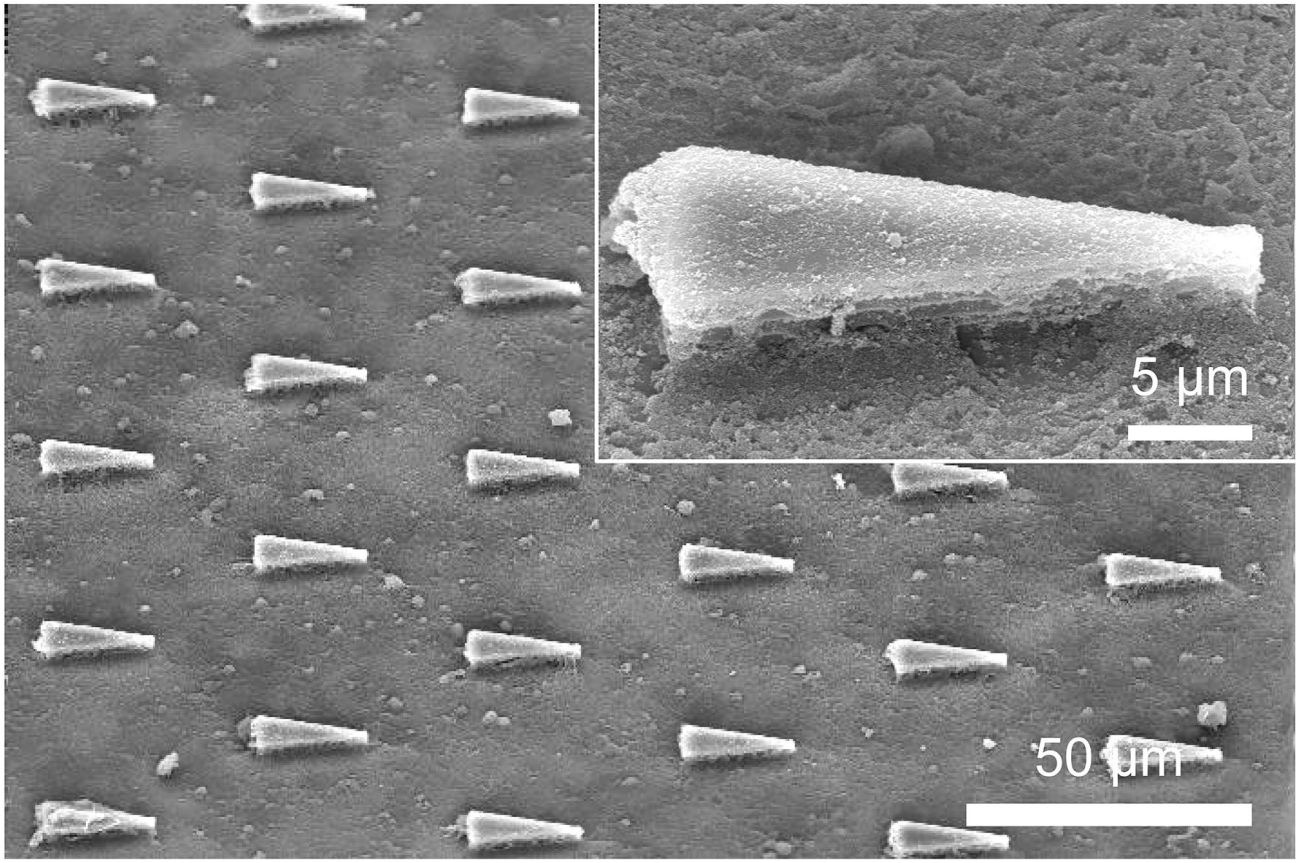

Fig. S8 Surface topography of CS6, the whole surface including the wedge-shaped bump arrays is coated with superhydrophobic Nanocoatings.

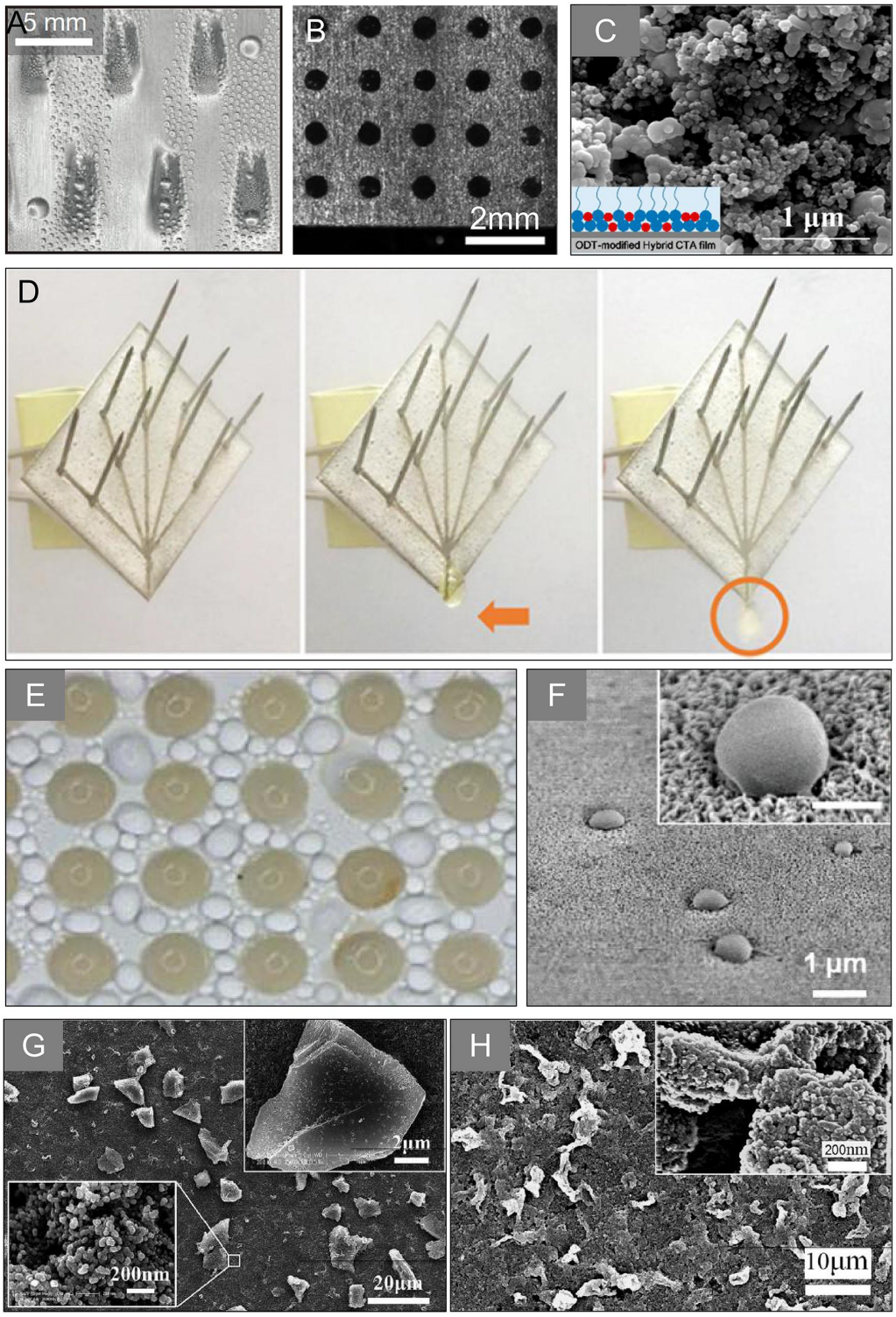

Fig. S9 Surface topography and structure for the beetle-inspired water collecting surface mentioned in the comparative references. (A) Slippery surface with asymmetric bump arrays[1]. (B) Integrative bioinspired surface with wettable patterns and gradient[6]. (C) Desert beetle-inspired superhydrophilic/superhydrophobic patterned cellulose film[7]. (D) Beetle-inspired hierarchical antibacterial interface[8]. (E) Bioinspired polydopamine coating with hydrophilic bump arrays[9]. (F) Scanning electron micrograph showing the morphology of a nanostructured aluminum substrate and randomly scattered nylon particles. Inset shows the zoom-in view of a single nanobump[10]. (G) Hybrid wetting surface with polymer-wrapped particles[11]. (H) Hybrid wetting surface with superhydrophilic TiO_2 nanoparticles[12].

Supplementary Movies

Movie S1: Side view of directional droplets coalescence and jumping on the BCI surface. Oblique droplet jumping and directional droplet transport on the BCI surface are captured by the high-speed camera, and the jumping drop with diameter of ~151 μm. After 307.50 ms, the jumping droplet moved ~4127 μm (about 4 mm) along the PD, and the diameter of the jumping droplet increased to ~654 μm due to the continuous droplets coalescence. The frame rate is 4000 fps with a shutter speed of 1/4000 sec and the movie playback speed is 30 fps.

Movie S2: Top view of directional droplets coalescence and jumping on the BCI surface. The jumping droplet with a diameter of ~80 μm, and its initial lateral velocity is ~0.01 m/s. After then, the jumping droplet coalesces with other drops and continue to jump along the PD, and a bigger drop with diameter of ~105 μm stays on the surface after 35.00 ms. The frame rate is 4000 fps with a shutter speed of 1/4000 sec and the movie playback speed is 15fps.

Movie S3: Top view of droplets directional moving and jumping on the BCI surface. Tiny droplets nucleate on the surface of the wedge-shaped bump, and as the droplets grow, they move along the unsymmetrical bump directionally and gather at the tail of the bump. The movie is observed using a stereomicroscope (Navitar, NY, USA) and the playback speed is 15 fps. During this process, the environmental temperature, the cooling stage temperature and the relative humidity is 20±3 ºC, ~2 ºC and 80±5%, respectively.

Movie S4: Top view of numbers of droplets coalescence and jumping on the BCI surface. When the droplets on the wedge-shaped bumps grow to reach the critical coalescence size, the droplets on the neighbouring bumps coalescence with each other and jump to departure from the BCI surface. The movie is observed using a stereomicroscope (Navitar, NY, USA) and the playback speed is 15 fps. During this process, the environmental temperature, the cooling stage temperature and the relative humidity is 20±3 ºC, ~2 ºC and 80±5%, respectively.

Movie S5: Side view of droplets coalescence and jumping in the vertical direction. When the sample is placed vertically and the wedge tip of the bump is pointing upward, the droplet is not only driven by the Laplace pressure gradient and gravity, but also can be removed by self-repelled droplets coalescence and jumping, which improved the droplet removal efficiency of the BCI surface, effectively. The frame rate is 4000 fps with a shutter speed of 1/4000 sec and the movie playback speed is 15 fps.

References

1 K. Park, P. Kim, A. Grinthal, N. He, D. Fox, J.C. Weaver and J. Aizenberg, *Nature*, 2016, **531**, 78-82.
2 D. Li, C. Qian, S. Gao, X. Zhao and Y. Zhou, *Int. J. Refrig*, 2017, **79**, 25-38.
3 Y. Xiu, L. Zhu, D.W. Hess and C.P. Wong, *J. Phys. Chem. C.*, 2008, **112**, 11403-11407.
4 J. Tian, J. Zhu, H. Guo, J. Li, X. Feng and X. Gao, *The journal of physical chemistry letters*, 2014, **5**, 2084-2088.
5 J. Liu, H. Guo, B. Zhang, S. Qiao, M. Shao, X. Zhang, X. Feng, Q. Li, Y. Song, L. Jiang and J. Wang, *Angew. Chem. Int. Ed.*, 2016, **55**, 4265-4269.
6 Y. Xing, W. Shang, Q. Wang, S. Feng, Y. Hou and Y. Zheng, *Acs Appl. Mater. Inter.*, 2019, **11**, 10951-10958.
7 C. Xu, R. Feng, F. Song, X. Wang and Y. Wang, *Acs Sustain. Chem. Eng.*, 2018, **6**, 14679-14684.

8 C. Wen, H. Guo, H. Bai, T. Xu, M. Liu, J. Yang, Y. Zhu, W. Zhao, J. Zhang, M. Cao and L. Zhang, *Acs Appl. Mater. Inter.*, 2019, **11**, 34330-34337.
9 P. Moazzam, H. Tavassoli, A. Razmjou, M.E. Warkiani and M. Asadnia, *Desalination*, 2018, **429**, 111-118.
10 Y. Hou, Y. Shang, M. Yu, C. Feng, H. Yu and S. Yao, *Acs Nano*, 2018, **12**, 11022-11030.
11 X. Wang, J. Zeng, X. Yu and Y. Zhang, *J. Mater. Chem. A*, 2019, **7**, 5426-5433.
12 X. Wang, J. Zeng, X. Yu, C. Liang and Y. Zhang, *Appl Surf Sci*, 2019, **465**, 986-994.